JOURNAL OF DEGRADED AND MINING LANDS MANAGEMENT
Volume 12, Number 4 (July 2025):8379-8390, doi:10.15243/jdmlm.2025.124.8379
ISSN: 2339-076X (p); 2502-2458 (e), www.jdmlm.ub.ac.id

Research Article

Flood inundation and damage assessment of the degraded Semliki River plains using SAR data, Google Earth Engine, and GIS techniques

Andrew Mulabbi[1,5], John Calvin Esagu[2*], Akello Gertrude[3], Turyahabwe Remigio[4]

[1] Department of Curriculum and Media Studies, Faculty of Education, Muni University, P.O Box 725, Arua, Uganda (amulabbi@muni.ac.ug)
[2] Department of Environmental Science, Faculty of Science, Kyambogo University, P.O Box 1, Kyambogo, Uganda
[3] Department of Geography, Faculty of Arts and Humanities, Kyambogo University, P.O Box 1, Kyambogo, Uganda
[4] Department of Geography, Faculty of Science and Education, Busitema University, P.O Box 236, Tororo, Uganda
[5] Department of Education, School of Education, Uganda Christian University, Besania Hill, Mukono

[*]corresponding author: calvinesagu1@gmail.com

Article history:
Received 27 March 2025
Revised 28 April 2025
Accepted 21 June 2025

Keywords:
flood depth
flood extent
flood impact
Google Earth Engine
Semliki
Sentinel-1

Abstract

The Semliki River valley in Ntoroko district has experienced devastating annual floods since 2019. Recurrent floods in Ntoroko District have displaced thousands and devastated pasturelands, disrupting livelihoods. Therefore, rapid assessment of flooded areas is crucial for developing effective mitigation strategies, disaster preparedness plans, and proactive policies to enhance resilience and mitigate the impact of future flood events. This study introduced a combined approach using Synthetic Aperture Radar (SAR) imagery and a digital elevation model (DEM) to map flood extent, depth, and building exposure in the Semliki Valley. Using Sentinel-1 SAR images taken both before and during the flood, combined with the ALOS PALSAR DEM, inundated areas and flood depths were determined, based on thresholding the SAR backscatter of the VH polarisation images. The flood extent maps were generated using Google Earth Engine and GIS techniques to create depth maps by subtracting the surface elevation from the height/surface of the flood waters. Building exposure and impact analysis for two flood events was ascertained through spatial join and overlay. The results showed that the 2023 flood event inundated approximately 1,968 hectares, including 1,553 hectares of pastureland and 74 buildings, while the 2024 event covered 1,139 hectares, equally inundating 1,050 hectares of pastureland and 54 buildings. Further analysis revealed that despite the smaller extent, the 2024 flood event caused a severe impact on the buildings compared to the 2023 flood disaster.

To cite this article: Mulabbi, A., Esagu, J.C., Gertrude, A. and Remigio, T. 2025. Flood inundation and damage assessment of the degraded Semliki River plains using SAR data, Google Earth Engine, and GIS techniques. Journal of Degraded and Mining Lands Management 12(4):8379-8390, doi:10.15243/jdmlm.2025.124.8379.

Introduction

Floods are among the most devastating natural disasters, causing widespread loss of life, property damage, and disruption of livelihood across the globe (Sellami and Rhinane, 2024). The problem of floods has been exacerbated by climate change and its associated impacts, like rising lake/sea levels, extreme weather events, and the melting of glaciers (Bhuyan et al., 2023). The impact is especially severe in resource-limited areas associated with poor preparedness and low resilience (Liu et al., 2024), where rapid detection and response are vital. According to the EMDAT disaster report (CRED et al., 2023) floods are recorded as the second frequent natural disaster and account for over 7700 deaths worldwide and over USD 100 million in economic losses. Southeast Asia and Africa account for the largest percentage of these fatalities and financial damages since they have been noted to be the most

affected regions due to climate change impacts. The transboundary Semliki River region in Ntoroko District, Uganda, is highly vulnerable to flooding due to its geography and weather patterns, worsened by inadequate execution of pre-flood mitigation strategies (Barasa et al. 2022). Located on the rift valley floor in the area between two major lakes (Edward and Albert) and at the base of the Rwenzori mountains, the region is prone to and experiences seasonal flooding, particularly during heavy rainfall (OPM-Uganda, 2016). Flooding in the Semliki valley is exacerbated by land degradation due to human activity, which exposes topsoil to erosion (Nkuba et al., 2021; Turyahabwe et al., 2024), leading to the depletion of the river banks. These recurrent floods create significant socio-economic and environmental problems, making effective flood monitoring and impact assessment crucial for disaster risk management and planning (Priyatna et al., 2023). Effective flood damage assessment necessitates the identification and quantification of elements at risk (EaR), including vulnerable communities, critical infrastructure, and ecological systems, to enhance disaster risk reduction strategies (Bhuyan et al., 2023). However, accurate flood impact assessment is curtailed by the high cost and logistical challenges of field surveys, which are often unfeasible until floodwaters recede. As a result, detailed documentation of flood events in tropical Africa remains scarce, with only 12% of the incidents thoroughly reported and recorded across the continent (CRED et al., 2023).

Remote sensing offers tools and techniques for rapid flood mapping and monitoring (Cohen et al., 2018; Hao et al., 2021; Tantri et al., 2024). Remote sensing sensors provide real-time and multitemporal imagery (optical and SAR) that captures flood information, given that floods are short-lived occurrences. However, clouds often obscure optical sensors (visible and near-infrared) during floods, limiting their usefulness (Klemas, 2015; Ge et al., 2020; Munawar et al., 2022). Synthetic Aperture Radar (SAR), with its all-weather, cloud-penetrating, day-night capabilities, can provide data in all seasons. SAR's multi-polarization data makes it easy to differentiate between flooded and non-flooded areas (Catalao et al., 2020; Ge et al., 2020). For this reason, many studies have used SAR data interpretation techniques to map flooded areas (Hossain and Meng, 2020; Hao et al., 2021; Mason et al., 2021; Ghouri et al., 2024). Common methods include image processing approaches like change detection based on backscatter, histogram thresholding, fuzzy classification, region growing, texture analysis, combined or hybrid approaches, and recently, machine learning and deep learning (Munawar et al., 2022). Using SAR data with advanced geospatial analysis in platforms like Google Earth Engine (GEE) and traditional Geographic Information Systems (GIS) allows for robust flood mapping and damage assessment (Nghia et al., 2022; Ariyani et al., 2024; Suni et al., 2024). Google Earth Engine's (GEE) cloud-based platform enables efficient and automated processing of large SAR datasets, and GIS facilitates spatial analysis and the integration of other relevant data for a complete flood assessment.

With the influx of many SAR satellites (e.g., ERS, Envisat, Sentinel-1, ALOS PALSAR, RadarSat, COSMO-SkyMed, and TerraSAR), a big chunk of open-source data is now made available. This has led to growing interest in research utilizing SAR data for mapping expeditions, including inundation mapping. Estimating and forecasting flood water depth is crucial for risk assessment and disaster mitigation, and SAR-based depth estimation is a popular research area (Cham et al., 2015; Cohen et al., 2018; Hao et al., 2021; Teng et al., 2022). Locally, flood mapping in Uganda has not been fully undertaken. A few studies have attempted to utilize remote sensing data for flood mapping in Uganda. Barasa and Wanyama (2020) mapped freshwater lake inundation, based on object-oriented classification, Erima et al. (2022) and Nedala et al. (2024), studied flood susceptibility and impact, respectively. The temporal resolution of satellite sensors can limit flood mapping due to issues like partial coverage or infrequent overpasses during floods. Given that river floods tend to recede quickly in most cases, sensors with low temporal resolution tend to miss such events, henceforth limiting the utility of remote sensing data in flood inundation and damage assessment.

Additionally, evaluating the exposure of elements at risk is crucial for disaster response planning, mitigation, and delivery of humanitarian aid. Population and buildings are the most affected elements at risk in both rural and urban floods (Zhu et al., 2020). Many studies have assessed building exposure to floods, but with an emphasis on urban floods (Mugume et al., 2024). Very little has been done about rural floods, yet rural populations are less resilient than their urban counterparts. For the case of Uganda and the Semliki Valley in particular, no studies exist concerning the use of SAR data for rapid assessment of flood damage, up till now the region continues to suffer from floods annually due to river bank erosion, land use change, melting of the glacier ice from the Mt. Rwenzori peak and rising water levels of lake Albert. This study sought to address these limitations by developing a rapid method for determining flood extent and depth using SAR data and a digital elevation model (DEM), and characterising building exposure based on flood depth levels suitable for areas with limited satellite coverage and advanced resources like speed boats and drone to carry out field-based assessment. The proposed workflow in this study builds upon existing techniques but offers several advantages. Primarily, it integrates SAR satellite data, high-resolution DEM, and Google building footprint data for a more complete picture of the flood events. It goes beyond exposure assessment

by conducting flood impact analysis based on flood depths. The May 2023 and August 2024 extreme flood events in Semliki Valley, Ntoroko district, serve as a case study. Google Earth Engine (GEE) and GIS are used to assess flooding and damage in the transboundary Semliki River region of Ntoroko District.

Materials and Methods

Description of the study area

The study was conducted along a section of the Semliki River floodplain in Bweramule sub-county, Ntoroko District, Uganda. The area is located in the western part of Uganda, on the floor of the western arm of the East African Rift Valley. Bweramule is one of the seven sub-counties in Ntoroko district (Figure 1). The Semliki River originates from Lake Edward to the south and flows into Lake Albert in the north. The river forms part of the border between Uganda and the Democratic Republic of the Congo. The upper part of the river flows through the heavily forested Semliki National Park, and the lower section winds through grasslands inhabited by the Batuku pastoral community before emptying its water into Lake Albert.

The Semliki River catchment area encompasses protected areas like Semliki National Park, Toro Wildlife Reserve, and Virunga National Park (DRC). This rich ecosystem attracts tourists interested in birdwatching, plant life, sport fishing, and wildlife viewing, including elephants, hippos, crocodiles, buffaloes, antelopes, and over 400 bird species (Kabenge et al., 2017).

The residents of this area are primarily engaged in small-scale subsistence farming and pastoralism, dealing with cattle and goats. Ntoroko District enjoys a year-round growing season thanks to its bimodal rainfall pattern. The first rainy season occurs from March to May, while the longer season stretches from August to November. Annual rainfall varies considerably, ranging from less than 800 to 1,600 millimetres, with higher elevations receiving more precipitation (Nkuba et al., 2019). Areas near the foot slopes of the Rwenzori Mountains experience reliable rainfall, enabling cultivation during both seasons. Temperatures vary significantly depending on altitude. The plains are hot, with temperatures reaching up to 25 °C. In contrast, the highlands can be quite cold, with temperatures dropping below freezing. Lowland humidity ranges from 72% to 80%, while the highlands are more humid, exceeding 80% (Bwambale et al., 2015).

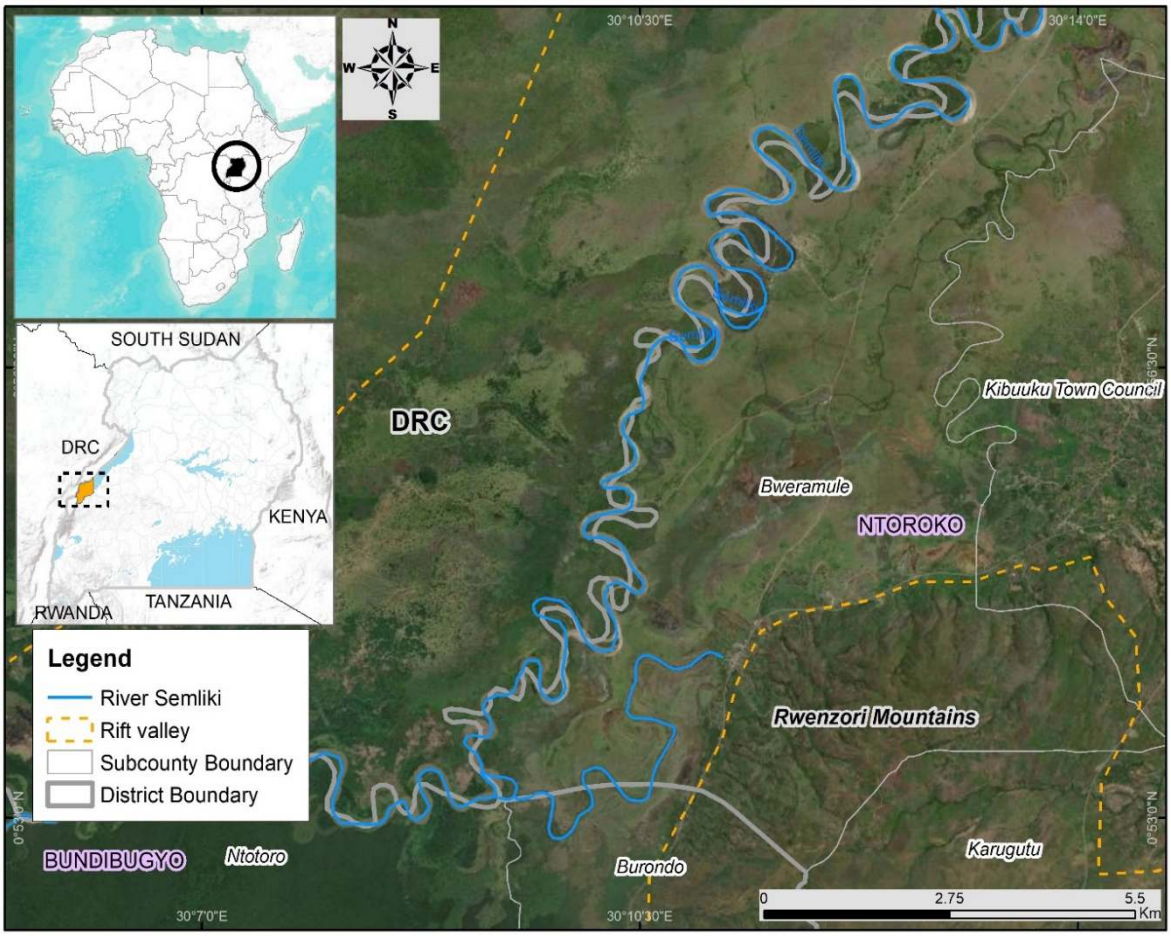

Figure 1. Location of the study area.

The topography is dominated by the Rwenzori Mountains and their eastern escarpments, which slope downwards toward Lake Albert. The Semliki valley is one of the lowest areas in Uganda, lying at a height of about 650 meters above sea level, and the adjacent escarpment sits at 1,700 meters above sea level. The landscape features numerous gorges and valleys, through which several major, permanent rivers flow, emptying their waters into the Semliki flats. The rivers carry varying amounts of sediment and boulders, depending on their volume and flow rate. The primary water sources for these rivers are the Rwenzori Mountains and the northern escarpments, characterized by rich tropical and riverine forest ecosystems. The soils in the Semliki River valley are primarily grey, alkaline alluvial clay sediments of low fertility, derived from Rift Valley deposits. Tectonic activity along the valley floor has resulted in igneous and metamorphic bedrock (mainly granites, gneisses, and schists) in the Rwenzori Mountains and escarpments (Link et al., 2010). These steep slopes provide the source material for the soil deposits found along the river. The rivers distribute gravel and sand across the valley before depositing finer sediments (sand and clay) into Lake Albert. The main soil types along the Semliki River include Pellic Vertisols, Mollic Andosols, Orthic Ferralsols, and Humic Gleysols. Livestock farming and fishing are the main economic activities in the area. Overgrazing in areas depletes the vegetation, leaving the river banks bare and susceptible to inundation. Given the location of the study area, i.e., in between two major lakes, being drained by many rivers, and being part of the western East African rift valley, the district is very prone to flooding caused by the rivers severely bursting their banks as well as rising water levels of Lake Albert

Data

This study utilised the Sentinel-1 GRD images for two flood events, i.e., May 2023 and August 2024. Two images (pre-flood and post-flood) with VH polarization and descending path for the two flood events were obtained. The VH polarization was prioritized due to its effectiveness in delineating flooded areas, particularly within vegetated regions, and its superior contrast over open water. The VH polarization is sensitive to surface roughness and is associated with fewer classification errors (Kianfar, 2019). A descending orbit path was selected for its favourable alignment with the study area's specific timing and conditions, ensuring the acquisition of consistent and optimized imagery for flood change detection. The Sentinel-1 data is chosen because it is not affected by weather conditions and is excellent for detecting changes in water surfaces due to its backscatter properties. These datasets were used to ascertain the extent of the two flood events in the study area. Additionally, the Global surface water (Pekel et al., 2016) accessed via Google Earth Engine (JRC/GSW1_0/GlobalSurfaceWater) was also used to mask the permanent water areas from the flood area. It contains data on the occurrence, seasonality, and global surface water extent from 1984 to 2020. The HydroSheds DEM data (Lehner and Grill, 2013) (WWF/HydroSHEDS/03VFDEM) was also used in this study for terrain analysis and eliminating slopes greater than 5% since they are unlikely to retain flood waters. A building footprint dataset (GOOGLE/Research/open-buildings/v3/polygons) provides high-resolution data on building footprints globally. Additionally, the ESA global land cover dataset (Zanaga et al., 2022) (ESA/WorldCover/v200/2021) was used to estimate the area of affected pastureland. For validation purposes, we used field assessment reports obtained from the Ntoroko District Disaster Management Committee and the Office of the Prime Minister (Kabenge et al., 2017)

Image processing

The sentinel-1 SAR ground range detected (GRD) data used in this study has already undergone preliminary pre-processing by the producer i.e., it is multi-looked, projected, calibrated, and provides georeferenced radar backscatter data in amplitude form, suitable for a wide range of applications like flood mapping, land cover analysis, and disaster monitoring. As such, pre-processing involved clipping the images as per the region of interest (ROI), filtering the images to select only the descending orbit path, thermal noise removal, speckle filtering using a smoothing radius of 50, chosen to balance speckle reduction, and preservation of detail. The derivation of the change difference images is the last step before undertaking further analysis. The descending orbit path is preferred since images are acquired in the morning and hence free from the impact of diurnal changes (Chen et al., 2016).

Flood mapping

The primary method for flood mapping in this study involved the application of a threshold to Sentinel-1 SAR backscatter values. This approach capitalizes on the capacity of SAR to discriminate between flooded and non-flooded surfaces based on variations in backscatter intensity. The threshold was determined based on trial and error, and this value can vary depending on the study area (Amitrano et al., 2024). We used two threshold values of 1.10 and 1.30 to differentiate flooded pixels from non-flooded pixels based on their backscatter values. The use of two thresholds was necessitated by the fact that the flood events occurred in different seasons, with the area having different surface conditions, e.g., the 2023 floods occurred in May, while the 2024 floods occurred in August, which is associated with a short dry season. Eyewitness accounts attest that these floods were caused by rains occurring far away in the mountains, on the Ugandan and the DRC sides. A change detection approach was employed, utilizing Sentinel-1 SAR imagery to map flood inundation.

Baseline backscatter values were established from pre-flood Sentinel-1 images. These were then compared to backscatter values from post-flood Sentinel-1 images, which captured changes during the flood event. A difference image, created by subtracting the pre-flood values from the post-flood values, highlighted areas of significant backscatter reduction, effectively identifying potentially flooded regions (Ge et al., 2020). To refine the change detection results, a water mask was applied to eliminate the permanent water areas from the flooded extent area. This ensures that only temporary water areas are classified as potentially flooded. It is worth noting that this method has some limitations, including misclassification, e.g., dense vegetation and wet soil may depict backscatter properties similar to those of open water bodies. This procedure was implemented in GEE based on a modified version of the schematic approach developed by UN-SPIDER, 2019 project (Wong et al., 2021). This recommended practice provides a user-friendly and efficient tool for generating flood data, accessible to all skill levels.

Flood damage and depth analysis

Flood extent is mapped as a binary mask based on raster pixels with 1 representing the flooded area and 0 for non-flooded. To compute the total flooded areas, flooded pixels are isolated from the non-flooded pixels. These are summed up, first into square meters determined by the spatial resolution of the image, and then converted into hectares. Flood damage assessment covered the aspects of pastureland, building exposure, and impact on the settlement area. Pastureland is preferred here since the area is part of the cattle corridor with cattle rearing as the main economic activity. During flood episodes, the pastureland is submerged, and livestock are left without grazing areas, which affects the health of the livestock and leads to economic losses. To ascertain the extent of affected pastureland, first, the grassland pixels are masked from the ESA land cover raster and then averaged with the flood extent raster through overlay, such that 1 represents grassland pixels that are flooded and 0 for non-flooded areas. The extent of the flooded grassland is calculated using the same procedure as for flood extent mapping. This procedure was implemented using Google Earth Engine (GEE).

After ascertaining the extent of the flooded areas, this was exported and used for further analysis in the ArcGIS environment to estimate the depth of the flooded areas. Flood depth within identified flood zones was calculated using the ALOS PALSAR DEM, downloaded from www.asf.alaska.edu/#/?dataseta. This DEM was preferred due to its global coverage and good spatial resolution. It is a precondition that the resolution of the DEM and the flood extent raster match to ensure accurate extraction of elevation values (Cham et al., 2015). The approach used in this study combines aspects from a procedure outlined by Cham et al. (2015) and Cohen et al. (2018). The procedure involves a pixel-by-pixel depth estimation based on the steps in (Figure 2) and these include; extraction of the flood extent boundary (polygon), conversion of the extent polygon into a polyline, generation of points along the flood boundary polyline, sampling the DEM at the points generated, interpolation of the elevation point values using the Triangular irregular network (TIN) to yield a flood water surface raster, using raster math to subtract the DEM from the flood water surface raster, and the output is a flood depth raster. Further processing involves clipping the extent raster using the flood depth raster. The flood depth map is classified using the natural breaks method into 4 classes, i.e., low, medium, high, and very high.

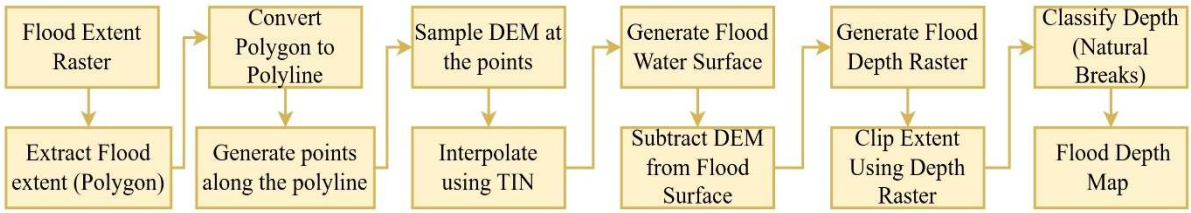

Figure 2. The flood depth mapping workflow using GIS.

Building exposure and impact analysis

An exposure analysis was conducted to determine the number of buildings affected by the flood waters in the study area. This was implemented using the GIS analysis tools 'intersect' and 'spatial join' to find the intersection between the flood extent and the buildings. All buildings intersecting with the flooded areas were identified as exposed buildings, including those only partially within the flood extent polygons. Further analysis was done to classify exposed buildings according to flood depth to establish the extent of impact suffered. Here, the spatial join was used to join exposed buildings to the different flood depth classes, and summary statistics were derived to indicate the number of buildings per flood depth class. Hence, exposed buildings are classified according to the level of impact, corresponding to the flood depth classes, namely, low, medium, high, and very high impact. Buildings in deep waters are regarded as high impact because the time taken for floods to recede also depends on the depth (Simpson et al., 2013). Those in the deep flood waters are likely to feel the impact for a long period and even incur higher costs to repair their buildings than those in low-impact areas.

Results

Flood extent and depth

Flood extent mapping for the section of the River Semliki in the Bweramule sub-county (Figure 3) was conducted based on the Sentinel-1 satellite imagery. Flood depth was then estimated using the ALOS PALSAR DEM. Figures 3 (b) and (c) illustrate the resulting flood extent and depth for the mapped area of the River basin on May 5th, 2023, and August 3rd, 2024. The study adopted a comparative approach by considering two flood events, i.e., 2023 and 2024.

The flood extent was mapped for the two years and compared to ascertain which flood event covered a larger area and resulted in greater damage or impact. The results show that the floods of 2023 affected a larger area, covering up to 1968 ha, while the 2024 event covered 1139 ha (Table 1).

Figure 3(a) shows the areas before the flood and after the flood in 2023 (b) and 2024 (c). The red colour indicates the estimated flooded area. It is observable that the flooded area extends over a large area on either side of the river, e.g., the Ugandan and the DRC side.

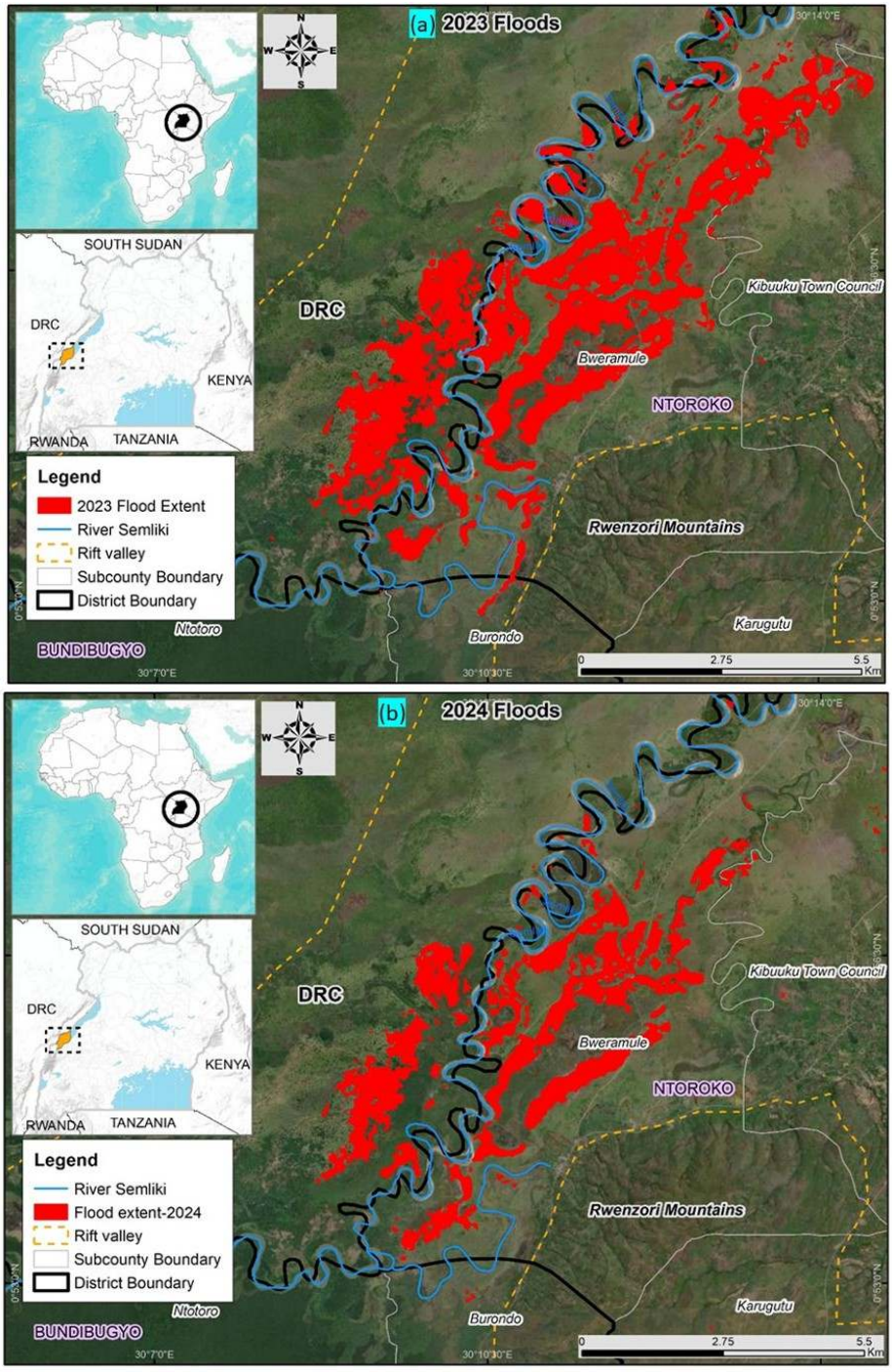

Figure 3. Flood extent for the two years under consideration: (a) 2023 and (b) 2024.

Flood depth analysis based on the ALOS PALSAR DEM reveals that most areas experienced floods with a depth of less than 0.5 meters. However, some localized areas (Figure 4a and b) experienced significantly deeper flooding, exceeding 1 meter. These deeper areas are generally located adjacent to the river channel and are likely associated with older levee formations and depressions. It is also noticeable that there are limited variations in flood depth, which could be attributable to the nature of the plains having the same elevation. The estimated flood extents were qualitatively validated using ground truth data collected by the field teams conducting a preliminary assessment post-flood. Photographs from several locations in Bweramule subcounty and Kibuuku town council, and impact reports from the Ntoroko District disaster management committee, served as ground truth. These photos suggest that most areas experienced flood depths of less than 0.5 meters (based on the height of people and houses in the images), which is consistent with the model's estimations (Figure 6).

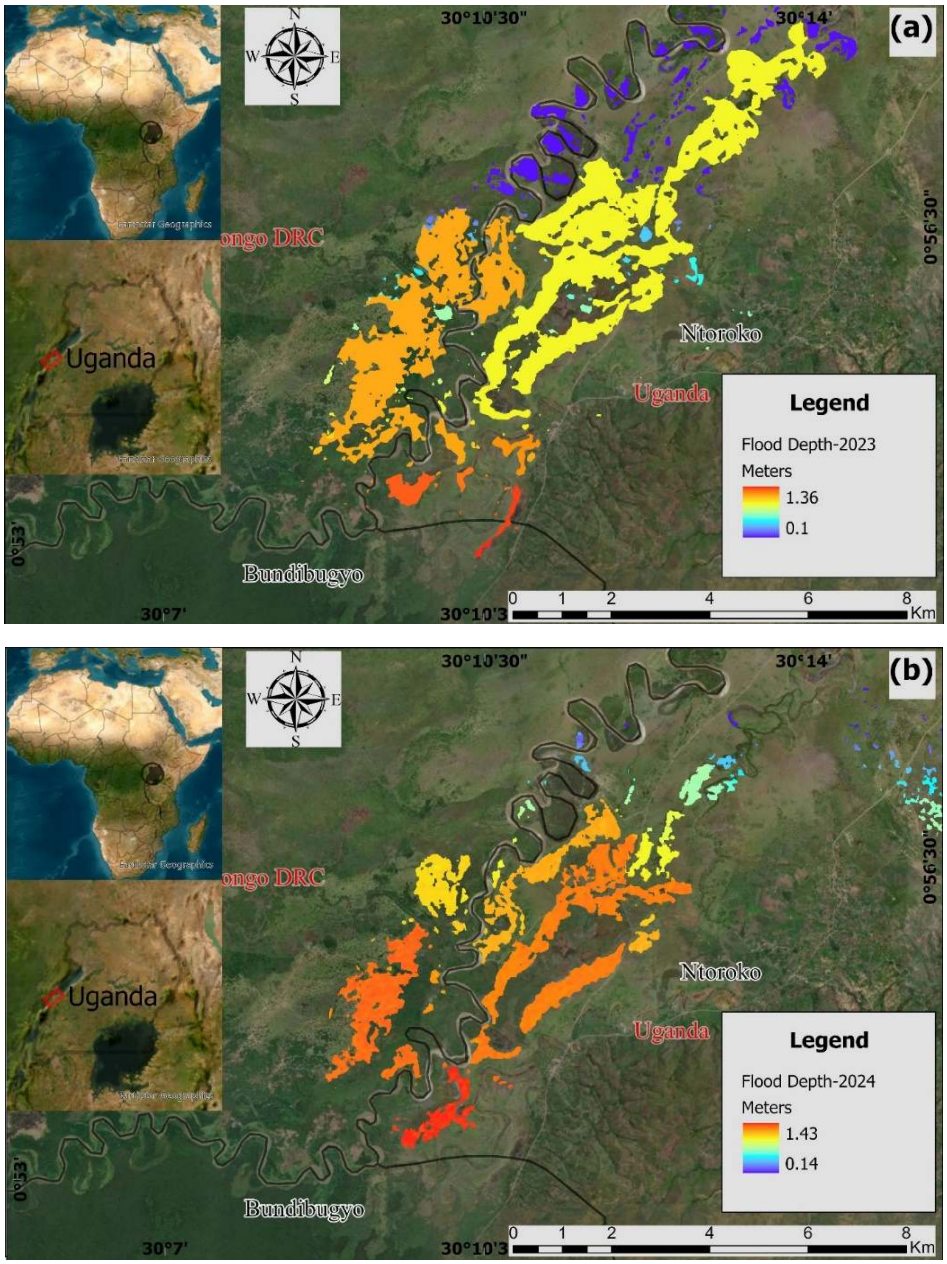

Figure 4. Flood depth for the years: (a) 2023, and (b) 2024.

Flood damage

Flood damage assessment in this study covered the impact on pastureland, buildings, and settlement areas. This was ascertained by comparing pre-flood and post-flood images. The pre-flood image served as the baseline for change detection, and from the difference images, we calculated the extent of damage caused by the two flood events. The results indicate that 1,553 ha of pastureland were submerged by floodwaters in

2023, and in 2024, an estimated 1,050 ha of pastureland were affected. Due to the flat terrain in this area, floodwaters can persist for several weeks before the pastureland is available again for grazing. Based on ESA global land cover data, the settlement area impacted by the flood is estimated at 74 ha and 13 ha in 2023 and 2024, respectively. It is noticeable that the 2023 flood event caused more widespread damage than the 2024 event, given that more pastureland, settlement area, and buildings were affected. The number of exposed buildings also varies between the two flood events (Table 1 and Figure 5), specifically, 71 and 54 buildings for 2023 and 2024, respectively. Given the large extent of affected pastureland, the region's agricultural sector is significantly impacted. Flooded pastureland can severely affect the local economy, food supply, and the livelihoods of farmers and their communities since, during such episodes, livestock do not feed well, impacting their health and milk production.

Table 1. Comparative analysis between 2023 and 2024 flood events.

Effect	2023	2024
Flood extent (ha)	1,968	1,139
Pastureland (ha)	1,553	1,050
Exposed buildings	71	54
Settlement area (ha)	74	13

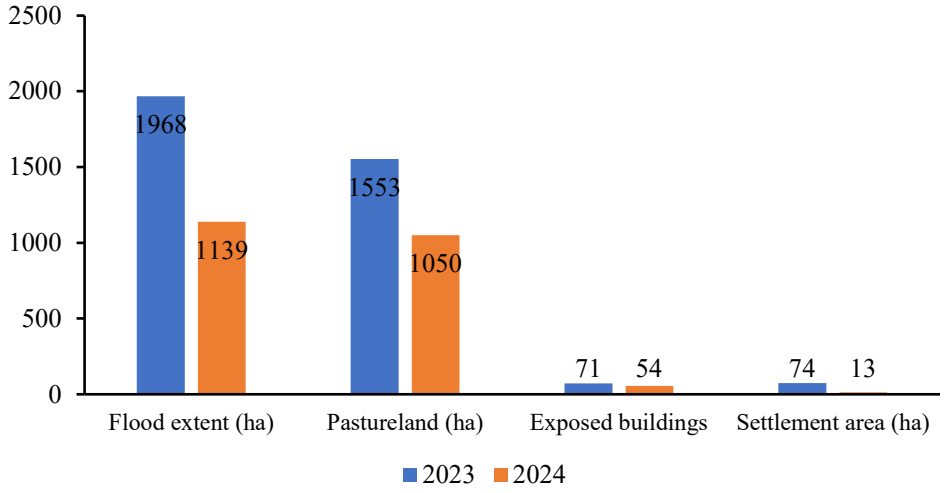

Figure 5. Statistics of flood extent, affected pastureland, exposed buildings, and settlement area for the two flood events.

Figure 6. Field photos taken post-flood in Bweramule Subcounty.

Flood impact on buildings

Analysing the extent of impact on buildings at each flood risk level is crucial for effective flood damage prevention and monitoring. It is also important in flood disaster response planning, including the delivery of humanitarian aid. This study based the flood impact analysis on the flood depth aspect, which directly impacts the flood recession period and the potential financial loss incurred to repair the buildings after the flood (Chen et al., 2016). The results are shown in Figure 6. The statistics indicate that most of the exposed buildings during the 2023 event are situated in low-depth zones. Only 17 buildings were found to be in the high-risk zones. In 2024, many exposed buildings are situated in the medium flood depth zone. Only 5 buildings were found to be located in the low-risk zone. This implies that the 2024 flood event had a greater impact on building damage than the 2023 event.

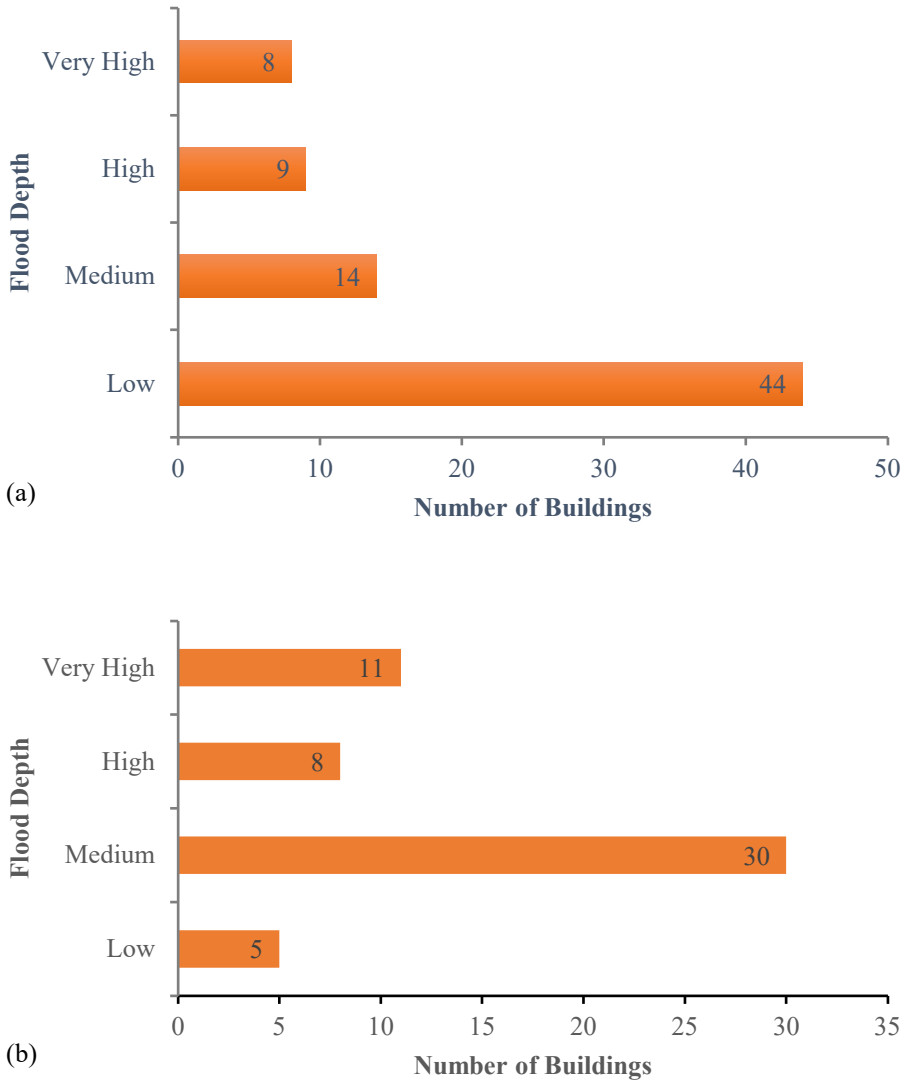

Figure 7. Flood impact on Buildings for the years 2023 (a) and 2024 (b).

Discussion

This study effectively demonstrates the utility of Sentinel-1 SAR data and change detection/thresholding algorithms for mapping floods in the Semliki Valley, Uganda. The findings provide valuable insights into the spatial extent of inundation, the settlement area affected, and the impacts on pastureland and buildings. These results can inform improved flood management strategies, support decision-making, and enhance community resilience in flood-prone regions. Ultimately, this research significantly contributes to flood management and preparedness efforts in Ntoroko, Uganda. By providing precise flood maps, authorities can create better strategies to mitigate flood damage, respond to floods more effectively, and devise targeted interventions to combat land degradation in the study area. These strategies include early warning systems, evacuation plans, wetland restoration plans, and improvements to infrastructure. Information about flooded pastureland can help governments make agricultural and land use policies and dispatch aid to affected farmers due to floods (Nkuba et al., 2021). The Sentinel-1 satellites have been acquiring images at good temporal and spatial resolution, rendering them very useful for the swift and timely mapping of floods (Bernet et al., 2018).

The flood extents between the two years vary, with 2023 showing a larger potentially flooded area than 2024. This contrasts with field reports and eyewitness accounts stating that the 2024 flood event was the biggest in over 5 years. This discrepancy could be attributable to the limitations of the Sentinel-1 C band, i.e., the failure to differentiate between volume scattering and water backscatter (Mason et al., 2012; Ge et al., 2020; Munawar et al., 2022). It is very possible that some flooded but not submerged vegetation areas may have been missed by these images. Therefore, using methods and data sensitive to floods in vegetation areas is crucial to ascertain the exact extent of flooded areas in Bweramule sub-

county. However, such SAR data using the L-band, which can map surface conditions below the vegetation, is available at a fee. Nonetheless, data fusion approaches that combine Sentinel-1 data with other datasets could help improve the accuracy of these maps.

Semliki valley experiences frequent flooding due to climate change, deforestation, overgrazing, and snowmelt waters from the Rwenzori mountain glacier. These floods have devastating effects, impacting lives, livelihoods, and the entire socio-economic structure of the region (Barasa et al., 2022). During the flooding time, the pastoral farmers in the area are forced to move their livestock to new places, leading to land conflicts with other communities in the region (Nkuba et al., 2019) and encroachment on the protected conservation areas, leading to heavy penalties and prosecution by the government authorities (Nkuba et al., 2021). It is also worth noting that some of the pastureland loss is attributable to the shifting course of the Semliki River, which has been exacerbated by overgrazing of the river banks, rendering them highly susceptible to erosion.

There is a variation between the number of exposed buildings for the two years and the extent of impact encountered. Much as the 2023 flood event affected more buildings, the 2024 flood event had a greater impact on the buildings than the 2023 event. This is corroborated by the field reports and eyewitness accounts that indicated the 2024 floods were unprecedented in the recent past. The most affected buildings are those closest to the river and the wetlands in the area. This is because Rivers naturally act as drainage, making them prone to overflowing during heavy rainfall or storm surges (Sellami and Rhinane, 2024). The impact analysis considered only flood depths due to the difficulty of accessing detailed information about the building conditions, construction materials, and utilities. The accuracy of these results is also dependent upon the quality (confidence score) of the building footprint dataset used. As noted by Bhuyan et al. (2023) this dataset does not account for the latest buildings and those that have ceased to exist due to demolition. Hence, this contributes to the uncertainty of the results derived using the approach explained in this study. This analysis provides a valuable resource for understanding the area's flood vulnerability, enabling local government planners and emergency responders to create strategies that minimize flood risk and safeguard the community. It is also useful for planning strategies to combat land degradation in the region since it is considered one of the causes of frequent flooding.

Flood depth estimation based on DEM is dependent upon the quality of the DEM used, and therefore, overestimations might occur and create misleading results (Cohen et al., 2018). The river valley morphology and the resolution of the DEM also affect the estimation accuracy. High-resolution elevation data like LiDAR should be considered for more trusted results. Future research should consider developing a method for accurately mapping flooded vegetation using open-source datasets. Combining remote sensing results with field surveys so that information on building quality, status, and other elements at risk is captured in flood damage assessment to provide authorities with a more holistic situation report. Additionally, methods for assessing the effectiveness of the flood mitigation and wetland restoration measures in the study area are needed.

Conclusions

This research presents an approach for automatically and swiftly mapping floods using synthetic Aperture radar data. In an area like Semliki that floods during every rainy season, swift response is key, and yet it requires swift data acquisition. This study demonstrates the effectiveness of SAR satellite data for accurately mapping flood extent and the usefulness of Google Earth Engine for identifying damaged buildings; nonetheless, on-the-ground verification is necessary for complete accuracy. Analysing the level of impact on the exposed buildings also proved valuable for assessing flood impact, since such information helps to design targeted interventions in case of flood occurrence. There remains a need to propose methods that can accurately map floods in vegetation areas using SAR data. The resolution of the elevation data should be carefully considered to ensure accurate estimations. This research offers valuable insights into flood risk in Bweramule sub-county and can support disaster relief, inform flood mitigation strategies, and monitor recovery efforts.

Acknowledgement

The authors would like to appreciate the disaster management committee of Ntoroko district for providing the required information.

References

Amitrano, D., Di Martino, G., Di Simone, A. and Imperatore, P. 2024. Flood detection with SAR: A review of techniques and datasets. *Remote Sensing* 16(4):1-38, doi:10.3390/rs16040656.

Ariyani, D., Purwanto, M.Y.J., Sunarti, E., Perdinan, and Juniati, A.T. 2024. Integrated flood hazard assessment using multi-criteria analysis and geospatial modeling. *Journal of Degraded and Mining Lands Management* 11(4):6121-6134, doi:10.15243/jdmlm.2024.114.6121.

Barasa, B. and Wanyama, J. 2020. Freshwater lake inundation monitoring using Sentinel-1 SAR imagery in Eastern Uganda. *Annals of GIS* 26(2):191-200, doi:10.1080/19475683.2020.1743754.

Barasa, B., Nakileza, B., Mugagga, F., Nseka, D., Opedes, H., Gudoyi, P.M. and Ssentongo, B. 2022. Natural hazards magnitude, vulnerability, and recovery strategies in the Rwenzori Mountains, Southwestern Uganda. In: Adelabu, S., Ramoelo, A., Olusola, A.,

Adagbasa, E. (eds), *Remote Sensing of African Mountains*. Springer, Cham, doi:10.1007/978-3-031-04855-5_5.

Bernet, D.B., Zischg, A.P., Prasuhn, V. and Weingartner, R. 2018. Modeling the extent of surface water floods in rural areas: Lessons learned from the application of various uncalibrated models. *Environmental Modelling and Software* 109(August):134-151, doi:10.1016/j.envsoft.2018.08.005.

Bhuyan, K., Van Westen, C., Wang, J. and Meena, S.R. 2023. Mapping and characterising buildings for flood exposure analysis using open-source data and artificial intelligence. *Natural Hazards* 119(2), doi:10.1007/s11069-022-05612-4.

Bwambale, B., Bagampadde, U., Gidudu, A. and Martini, F. 2015. Seismic hazard analysis for the Albertine Region, Uganda – a probabilistic approach. *South African Journal of Geology* 118(4):411-424, doi:10.2113/gssajg.118.4.411.

Catalao, J., Raju, D. and Nico, G. 2020. Insar maps of land subsidence and sea level scenarios to quantify the flood inundation risk in coastal cities: The case of Singapore. *Remote Sensing* 12(2), doi:10.3390/rs12020296.

Cham, T.C., Mitani, Y., Fuji, K. and Ikemi, H. 2015. Evaluation of flood volume and inundation depth by GIS midstream of Chao Phraya River Basin, Thailand. In: *Sustainable Development* (pp.1049-1060), doi:10.2495/sd150912.

Chen, A.S., Hammond, M.J., Djordjević, S., Butler, D., Khan, D.M., and Veerbeek, W. 2016. From hazard to impact: flood damage assessment tools for megacities. *Natural Hazards* 82(2), doi:10.1007/s11069-016-2223-2.

Cohen, S., Brakenridge, G.R., Kettner, A., Bates, B., Nelson, J., McDonald, R., Huang, Y.F., Munasinghe, D. and Zhang, J. 2018. Estimating floodwater depths from flood inundation maps and topography. *Journal of the American Water Resources Association* 54(4):847-858, doi:10.1111/1752-1688.12609.

CRED, UCLouvain, and USAID. 2023. Disaster in Numbers. *Nature Medicine* 29(7):1857-1866. https://files.emdat.be/ reports/2023_EMDAT_report.pdf

Erima, G., Kabenge, I., Gidudu, A., Bamutaze, Y. and Egeru, A. 2022. Differentiated spatial-temporal flood vulnerability and risk assessment in lowland plains in eastern Uganda. *Hydrology* 9(11), doi:10.3390/hydrology9110201.

Ge, P., Gokon, H. and Meguro, K. 2020. A review on synthetic aperture radar-based building damage assessment in disasters. *Remote Sensing of Environment* 240(February):111693, doi:10.1016/j.rse.2020.111693.

Ghouri, A.Y., ur Rehman, A., Rasheed, F., Miandad, M. and Rehman, G. 2024. Flood mapping using the Sentinel-1 SAR dataset and application of the change detection approach technique (CDAT) to the Google Earth engine in Sindh Province, Pakistan. *Ecological Questions* 35(2):149-159, doi:10.12775/EQ.2024.024.

Hao, C., Yunus, A.P., Subramanian, S. and Avtar, R. 2021. Basin-wide flood depth and exposure mapping from SAR images and machine learning models. *Journal of Environmental Management* 297(April):113367, doi:10.1016/j.jenvman.2021.113367.

Hossain, M.K. and Meng, Q. 2020. A fine-scale spatial analytics of the assessment and mapping of buildings and population at different risk levels of urban flood. *Land Use Policy* 99(March):104829, doi:0.1016/j.landusepol.2020.104829.

Kabenge, M., Elaru, J., Wang, H. and Li, F. 2017. Characterizing flood hazard risk in data-scarce areas, using a remote sensing and GIS-based flood hazard index. *Natural Hazards* 89(3):1369-1387, doi:10.1007/s11069-017-3024-y.

Kianfar, N. 2019. The applicability of dual-polarized Sentinel-1 SAR data for the detection of flooded areas in pol-E Dokhtar, Lorestan, Iran. *International Archives of the Photogrammetry, Remote Sensing and Spatial Information Sciences - ISPRS Archives* 42(4/W18):655-657, doi:10.5194/isprs-archives-XLII-4-W18-655-2019.

Klemas, V. 2015. Remote sensing of floods and flood-prone areas: An overview. *Journal of Coastal Research* 31(4):1005-1013, doi:10.2112/JCOASTRES-D-14-00160.1.

Lehner, B. and Grill, G. 2013. Global river hydrography and network routing: Baseline data and new approaches to study the world's large river systems. *Hydrological Processes* 27(15):2171-2186, doi:10.1002/hyp.9740.

Link, K., Koehn, D., Barth, M.G., Tiberindwa, J.V., Barifaijo, E., Aanyu, K. and Foley, S.F. 2010. Continuous cratonic crust between the Congo and Tanzania blocks in western Uganda. *International Journal of Earth Sciences* 99(7):1559-1573, doi:10.1007/s00531-010-0548-8.

Liu, S., Zheng, W., Zhong, G., Zhen, Y., Han, Z. and Li, Y. 2024. Flood risk assessment of rural buildings in shouxihe basin based on vulnerability curve. *Tongji Daxue Xuebao/Journal of Tongji University* 52(1):68-76, doi:10.11908/j.issn.0253-374x.22211.

Mason, D.C., Bevington, J., Dance, S.L., Revilla-Romero, B., Smith, R., Vetra-Carvalho, S. and Cloke, H.L. 2021. Improving urban flood mapping by merging synthetic aperture radar-derived flood footprints with flood hazard maps. *Water (Switzerland)* 13(11), doi:10.3390/w13111577.

Mason, D.C., Davenport, I.J., Neal, J.C., Schumann, G.J P. and Bates, P.D. 2012. Near real-time flood detection in urban and rural areas using high-resolution synthetic aperture radar images. *IEEE Transactions on Geoscience and Remote Sensing* 50(8):3041-3052, doi:10.1109/TGRS.2011.2178030.

Mugume, S.N., Abasabyoona, G., Engwau, J., Sempewo, J., Van de Sande, B. and Butler, D. 2024. Assessment of the impact of the rise in Lake Victoria water levels on urban flooding using a GIS-based spatial flood modelling approach. *Urban Water Journal* 21(2):219-233, doi:10.1080/1573062X.2023.2284960.

Munawar, H.S., Hammad, A.W.A. and Waller, S.T. 2022. Remote sensing methods for flood prediction: A review. *Sensors* 22(3), doi:10.3390/s22030960.

Nedala, S., Puja, S., Kempango, L. and Ikendi, S. 2024. Assessing flood susceptibility and effectiveness of structural flood mitigation measures applied within Mubuku catchment in the Rwenzori Region, Uganda. *Natural Hazards* 1375-1397, doi:10.1007/s11069-024-06843-3.

Nghia, B.P.Q., Pal, I., Chollacoop, N. and Mukhopadhyay, A. 2022. Applying Google Earth Engine for flood mapping and monitoring in the downstream provinces of the Mekong River. *Progress in Disaster Science* 14(March):100235, doi:10.1016/j.pdisas.2022.100235.

Nkuba, M., Chanda, R., Mmopelwa, G., Kato, E., Mangheni, M.N. and Lesolle, D. 2019. The effect of climate information in pastoralists' adaptation to climate change: A case study of Rwenzori region, Western Uganda. *International Journal of Climate Change Strategies and*

Management 11(4):442-464, doi:10.1108/IJCCSM-10-2018-0073.

Nkuba, M.R., Chanda, R., Mmopelwa, G., Mangheni, M.N., Lesolle, D., Adedoyin, A. and Mujuni, G. 2021. Determinants of pastoralists' use of indigenous knowledge and scientific forecasts in the Rwenzori region, Western Uganda. *Climate Services* 23:100242, doi:10.1016/j.cliser.2021.100242.

OPM-Uganda. 2016. Ntoroko District: Hazard, Risk and Vulnerability Profile.

Pekel, J.F., Cottam, A., Gorelick, N. and Belward, A.S. 2016. High-resolution mapping of global surface water and its long-term changes. *Nature* 540(7633):418-422, doi:10.1038/nature20584.

Priyatna, M., Wijaya, S.K., Khomarudin, M.R., Yulianto, F., Nugroho, G., Afgatiani, P.M., Rarasati, A. and Hussein, M.A. 2023. The use of multi-sensor satellite imagery to analyze flood events and land cover changes using change detection and machine learning techniques in the Barito watershed. *Journal of Degraded and Mining Lands Management* 10(2):4073-4080, doi:10.15243/jdmlm.2023.102.4073.

Sellami, E.M. and Rhinane, H. 2024. A modern method for building damage evaluation using a deep learning approach - Case study: Flash flooding in Derna, Libya. *E3S Web of Conferences* 502:1-6, doi:10.1051/e3sconf/202450203010.

Simpson, S.C., Meixner, T. and Hogan, J.F. 2013. The role of flood size and duration on streamflow and riparian groundwater composition in a semi-arid basin. *Journal of Hydrology* 488:126-135, doi:10.1016/j.jhydrol.2013.02.049.

Suni, M.A., Rahmawati, A., Muis, H., Maarif, F. and Baharuddin, R.F. 2024. Flood vulnerability analysis using geographic information system in the core zone of the Lore Lindu biosphere reserve, Indonesia. *Journal of Degraded and Mining Lands Management* 12(1):6887-6897, doi:10.15243/jdmlm.2024.121.6887.

Tantri, O., Sampurno, J. and Adriat, R. 2024. Utilization of Sentinel-1 imagery for mapping the distribution of floods in the Putussibau Kota Subdistrict and Surrounding Areas. *Jurnal Geografika (Geografi Lingkungan Lahan Basah)* 5(1):76, doi:10.20527/jgp.v5i1.12779.

Teng, J., Penton, D.J., Ticehurst, C., Sengupta, A., Freebairn, A., Marvanek, S., Vaze, J., Gibbs, M., Streeton, N., Karim, F. and Morton, S. 2022. A comprehensive assessment of floodwater depth estimation models in semiarid regions. *Water Resources Research* 58(11):1-19, doi:10.1029/2022WR032031.

Turyahabwe, R., Andama, E., Mulabbi, A. and Nakiyemba, A. 2024. Understanding the nexus between traditional brick-making, biophysical and socio-economic environment of Goma Division, Mukono Municipality, Central Uganda. *Journal of Degraded and Mining Lands Managemen*, 11(4):6367-6378, doi:10.15243/jdmlm.2024.114.6367.

Wong, I., Hertel, V. and Botez, R. 2021. UN-SPIDER Recommended Practices for Exposure Mapping, Flood Hazard Mapping, and Flood Mapping: "Space-based Solutions for Disaster Risk Management and Emergency Response in Nigeria." April. www.unoosa.org

Zanaga, D., Van De Kerchove, R., Daems, D., De Keersmaecker, W., Brockmann, C., Kirches, G., Wevers, J., Cartus, O., Santoro, M. and Fritz, S. 2022. ESA WorldCover 10 m 2021 v200.

Zhu, S., Dai, Q., Zhao, B. and Shao, J. 2020. Assessment of population exposure to urban flood at the building scale. *Water (Switzerland)* 12(11):1-14, doi:10.3390/w12113253.